Heliyon 9 (2023) e20521

Contents lists available at ScienceDirect

Heliyon

journal homepage: www.cell.com/heliyon

Design and fabrication of gelatin-based hydrogel loaded with modified amniotic extracellular matrix for enhanced wound healing

Lifa Chen [a,1], JueLan Ye [b,1], Chong Gao [a], Fei Deng [a], Wei Liu [c,**], Qiang Zhang [a,*]

[a] The Department of Burn & Plastic Surgery, The Affiliated Hospital of Yangzhou University, Yangzhou University, 368 Hanjiang Middle Road, Yangzhou, Jiangsu, 225009, PR China
[b] Wuxi School of Medicine, Jiangnan University, Wuxi, Jiangsu, 214122, PR China
[c] The Affiliated Suqian First People's Hospital of Nanjing Medical University, 120 Suzhi Road, Suqian, Jiangsu, 223812, PR China

A B S T R A C T

Trauma can damage the structural integrity of skin leading to its function being affected. There is an urgent clinical need for innovative therapeutic wound dressings. However, several challenges persist despite the current demands. The development and application of functional dressings offer a novel approach to address skin and subcutaneous soft tissue defects. Amniotic membrane as an ideal biological multifunctional material covering wound surface has been reported in clinic. However, current clinical applications of amniotic membrane still have limitations, such as thinness and mechanically weak. In this paper, we employed decellularized human amniotic membrane (dHAM) as a bioactive extracellular matrix (ECM) and modified it through methacrylate (MA) grafting for engineering purposes, resulting in the photosensitive dECMMA. Subsequently, we utilized a photosensitizer to achieve photopolymerization of dECMMA with GelMA hydrogel, successfully creating a novel composite hydrogel termed dECMMA/GelMA. This composite hydrogel not only inherits the favorable physicochemical properties of hydrogels but also maintains comparable levels of bioactivity to dHAM itself, supporting cell proliferation, migration, angiogenesis, and retaining significant anti-inflammatory capacity.

Additionally, we evaluated the reparative effect of the designed dECMMA/GelMA composite hydrogel on rabbit wound defects. We demonstrated that the dECMMA/GelMA promoted wound healing and re-epithelization. These findings highlight the substantial benefits and therapeutic potential of the dECMMA/GelMA composite hydrogel as a practical solution for clinical applications in the treatment of soft tissue damage. Furthermore, this research provides a new strategy for designing and manufacturing bioactive dressings with exceptional clinical efficacy in the future.

1. Introduction

Trauma (including burns, acute injuries, etc.), as a type of disastrous and accidental event, not only occurs in war but also frequently in daily life, such as car accidents, fights, industrial injuries, waste fluids (water, oil, soup), hot metals, flames, steam, etc., which can all become the cause of injury [1]. Trauma can result in the disruption of the skin's structural integrity, resulting in impaired function and the appearance of skin defects or wounds [2]. Wound management is a major challenge faced by the global healthcare system. Currently, the use of dressings for the treatment of skin wounds is a highly effective method in clinical practice, and the dressings mainly include non-woven dressings, medicated moist dressings, tissue engineering substitutes, biologically-based dressings, biological and naturally derived dressings, as well as various combinations thereof [3,4]. However, the application of various dressings

* Corresponding author.
** Corresponding author.
E-mail addresses: m13813182298@163.com (W. Liu), ydzhangq@126.com (Q. Zhang).
[1] These authors contributed equally to this work.

https://doi.org/10.1016/j.heliyon.2023.e20521
Received 18 June 2023; Received in revised form 21 September 2023; Accepted 27 September 2023
Available online 28 September 2023

is also limited by their inherent material characteristics. At present, there is a strong desire in clinical work to have new strategies to achieve accelerated wound healing [5,6].

Although there is an urgent need for novel therapeutic wound dressings in clinical practice, there are also many challenges behind this demand [7]. A good dressing should be designed to have biological activity, such as inherent biological activity or bioactive components (drugs) incorporated into the dressing that can be released in the wound area. This dressing can directly interact with the wound surface during the wound healing process and have a beneficial impact on promoting tissue regeneration [8,9]. However, traditional dressings cannot restrict the evaporation of moisture from the wound surface, causing dehydration of the wound bed, and with increasing evaporation, traditional dressings adhere to the wound, causing severe pain when changing dressings [10,11]. With the deepening of interdisciplinary research between biomedical and materials science, various forms of wound dressings, such as sponges, foams, hydrogels, micro-needle patches, and sprayable liquids, have been developed and applied to wounds to solve problems encountered in the repair process. Among them, hydrogels have garnered the interest of numerous researchers owing to their biomimetic ECM structure, ability to maintain moisture and breathability, adjustable mechanical properties, and benefits for cell adhesion and proliferation [11,12].

One of the most widely used materials in hydrogel systems is methacrylated gelatin (GelMA), which is a double-bond modified gelatin that can be crosslinked and solidified into a gel through UV and visible light under the action of photoinitiator [13]. GelMA exhibits characteristics of both natural and synthetic biomaterials, featuring a three-dimensional structure conducive to cell growth and differentiation, exceptional biocompatibility, and favorable cellular response properties [14,15]. Furthermore, GelMA exhibits favorable temperature-sensitive gel properties and degradability, along with customizable mechanical properties that offer a range of viscoelastic characteristics. Consequently, it has found extensive application in the development of hydrogel-based wound dressings [13,14]. However, due to the complexity of the wound environment, the biological activity of most single hydrogel wound dressings is insufficient to rapidly promote wound healing, and components that promote epidermal tissue regeneration, neovascularization, collagen deposition, and other functions must be added to the hydrogel to accelerate healing by enhancing wound tissue regeneration performance [16–18].

Human decellularized amniotic membrane (dHAM) is a collagen-based extracellular matrix (ECM) derived from the human placenta, which is easily obtained, cost-effective, and biocompatible. dHAM is a natural material type of dressing [19]. Recent studies have demonstrated that the amniotic membrane contains a variety of growth factors, including fibroblast growth factor (FGF), epidermal growth factor (EGF), platelet-derived growth factor (PDGF), vascular endothelial growth factor (VEGF), and hepatocyte growth factor (HGF). These factors can promote the recruitment of human mesenchymal stem cells, epithelial formation, the development of new blood vessels, and the proliferation of dermal fibroblasts [20,21]. The HAM has demonstrated ideal effects in promoting

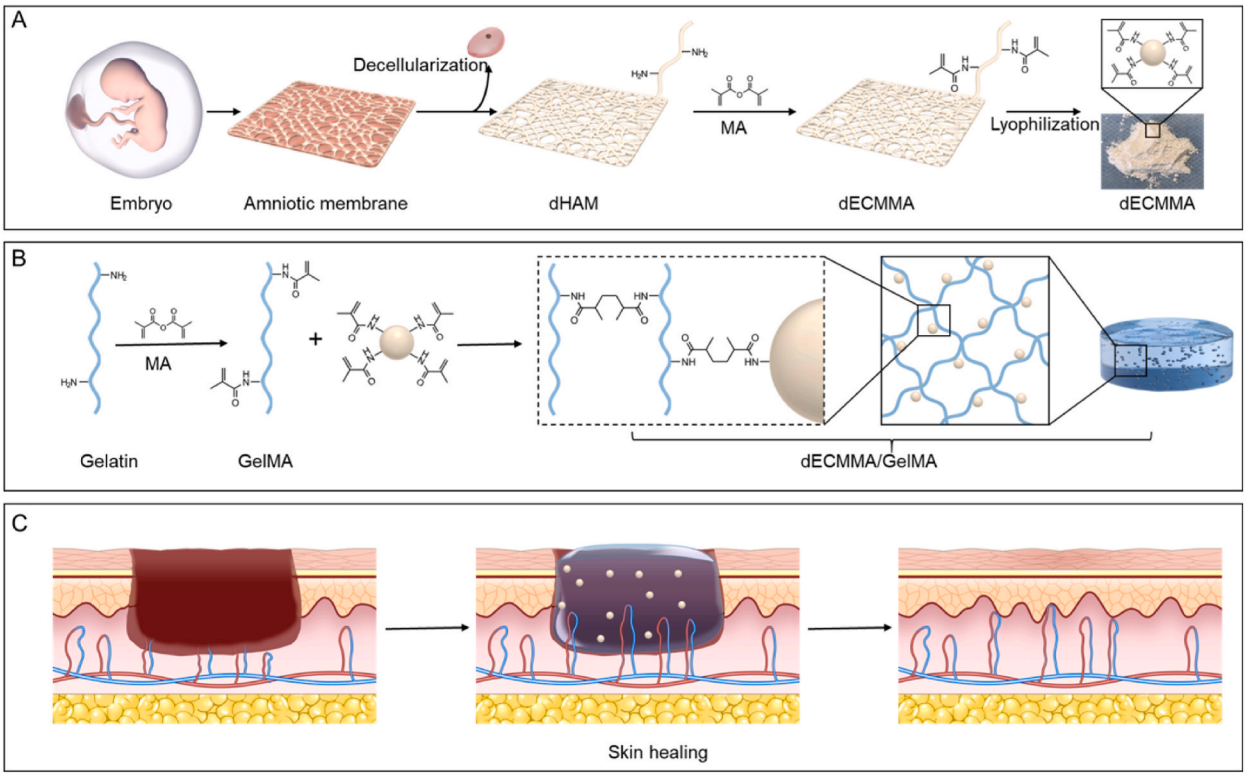

Fig. 1. Schematic illustrating the preparation process of the dECMMA/GelMA dressing for skin defect repair. A) Illustration of dECMMA preparation; B) Schematic preparation of dECMMA/GelMA; C) dECMMA/GelMA was used to cover skin defect to promote healing.

wound healing, reducing scars, and improving the damaged skin microenvironment [21]. Over the past few decades, the potential of amniotic membrane in treating wounds has been demonstrated through transplanting amniotic tissue to wounds [22–24]. However, completely attaching the amniotic membrane to the wound bed is very challenging because the membrane is relatively thin, smooth, soft, and mechanically weak, making it difficult to remain in place for a long time, limiting its widespread clinical application [25,26].

With the development of tissue engineering technology, material modification and biomaterial composite technology have been used to improve the performance of functional additives and overcome the limitations of single application efficacy [25,27,28]. In this study, we modified dHAM and gelatin through MA to prepare light-sensitive dECMMA and GelMA, respectively. We then constructed a functional composite hydrogel of dECMMA/GelMA by UV crosslinking dECMMA and GelMA. The physicochemical properties of dECMMA/GelMA were investigated, and the in vitro cellular toxicity, proliferation, migration, secretion, and angiogenic potential were evaluated. Finally, we conducted in vivo experiments to assess the wound healing-promoting ability of dECMMA/GelMA by covering the skin defect with the hydrogel (Fig. 1).

2. Materials and methods

2.1. Preparation of dECMMA

To prepare dECMMA, 10 mg/mL dHAM was stirred in a 1 mg/mL solution of New Zealand rabbit pepsin and 0.5 M acetic acid was added. The mixture was stirred for 48 h at room temperature. To precipitate the dissolved ECM components, 20% w/v NaCl was introduced, and then the mixture underwent centrifugation at 3000 rpm for 15 min at 4 °C. The resulting supernatant was then dialyzed for two days. The dECM was dissolved in 0.5 M acetic acid to a concentration of 10 mg/mL, and the pH was adjusted to 8–9 using NaOH. The solution was then reacted with MA (methacrylic anhydride) for 24 h. The resulting product was loaded into a dialysis bag with a molecular weight cutoff of 3500 and subjected to dialysis for a duration of two days. Subsequently, it underwent lyophilization to yield dECMMA [29].

2.2. Synthesis of GelMA hydrogel

Add 100 mL of deionized water to 10 g of gelatin powder and stir to dissolve in a constant temperature water bath at 60 °C. Under light-shielding conditions, mix methyl methacrylate anhydride with the gelatin solution at a rate of 1 mL/min at 60 °C with stirring at 300 rpm. After the mixture is homogeneous, dilute the reaction with 500 mL of deionized water at 50 °C, and then transfer it into a dialysis bag with a molecular weight of 14 kDa. The dialysis bag is rotated in a deionized water bath at 50 °C for 1 week with the water changed every 4 h. Then, the sample is frozen at −80 °C overnight, lyophilized, and stored at −4 °C for future use [18].

2.3. Preparation of dECMMA/GelMA

Preparation of 10% GelMA and 10% dECMMA solutions were carried out. 5 mL of each prepared GelMA and dECMMA solutions were taken in a small beaker, and stirred with a magnetic stirrer under dark conditions for 30 min. After the solutions were mixed evenly, they were sonicated for 0.5 h to remove bubbles. After degassing, the initiator, benzyl-2,4,6-trimethylbenzoylphosphinate (LAP, 5 mg/10 mL , Tokyo Chemical Industry, Japan) was added to the sample. The photosensitive dECMMA/GelMA hydrogel material was cured by exposure to ultraviolet light, followed by freeze-drying.

2.4. Characterization of dECMMA/GelMA

2.4.1. Scanning electron microscopy (SEM)

400 μL of the precursor solution was added into each well of a 48-well plate, and then the plate was exposed to light until the gel was fully formed. The gel was then frozen at −20 °C and the samples were placed in a freeze-dryer and left overnight. The freeze-dried samples were cut open with a sharp knife to expose the interior of the gel, and the surface was coated with gold before being observed by SEM [9,18].

2.4.2. Infrared detection

The hydrogel samples were freeze-dried and an appropriate amount of the freeze-dried hydrogel samples were ground and tested using the KBr pellet method. The chemical composition was determined using a Nicolet Nexus 670 FTIR spectrometer. The scanning test range was from 400 cm^{-1} to 4000 cm^{-1}, and the instrument testing resolution was 4 cm^{-1} [4].

2.4.3. Swelling experiment

1 mL of the precursor dECMMA/GelMA gel solution was taken and placed into a 24-well plate. The solution was then exposed to UV light until it completely gelled. The weight was recorded as W_0. The gel was then immersed in ultra-pure water for 0.5, 1, 2, 4, 8, 12, and 24 h, respectively. After removing the gel, the surface water was dried with filter paper, and the weight was recorded as Ws. The swelling ratio (SR) was calculated as follows: $SR = (Ws\text{-}W_0)/W_0 \times 100\%$ (Ws is the weight of the water-swollen gel at different time points, and W_0 is the weight of the fully gelled gel).

2.4.4. Mechanics experiment

The swelling balanced GelMA and dECMMA/GelMA hydrogel (10 mm in diameter and 5 mm in height) was tested for its mechanical properties with an Electric Dynamic Test System (M − 3000, Care measurement and control). The hydrogel was squeezed at a compression rate of 1 mm/min at room temperature until the rupture of the hydrogel [4,25].

2.5. In vitro studies

2.5.1. CCK8

100 μl of precursor dECMMA/GelMA gel solution (n = 6) was placed in a 96-well plate and exposed to ultraviolet light to solidify the gel. Logarithmic phase cells were digested with 0.25% trypsin to prepare a suspension of RAW264.7 cells (Stem Cell Bank, Chinese Academy of Sciences) with density of 5×10^4/mL. After adding 100 μl of cell suspension to each well, the plate was incubated in a constant-temperature cell culture incubator at 37 °C with 5% CO_2. CCK-8 (Boster, China) assays were performed on day 1, day 3, and day 5. In particular, the initial cell culture medium was aspirated and replaced with fresh medium, after which 10 μl of CCK-8 solution was added to each well. Following a 3-h incubation period, the absorbance at 450 nm was determined using a spectrophotometer [30].

2.5.2. Cell scratch assay

dECMMA/GelMA was loaded onto the bottom of a 24-well plate by freeze-drying. RAW264.7 cells suspension were seeded at a density of 3×10^4 cells/cm^2 on the surface of the well bottom and allowed to adhere and form a monolayer. Four evenly spaced horizontal lines were scratched onto the cell monolayer using a sterile 20 μL pipette tip, with approximately 1 cm distance between each line. The cells were washed three times with PBS to remove the scratched cells. The three groups of cells were then incubated at 37 °C and 5% CO_2 for 0 and 12 h. Microscopic images were taken at both time points to observe the closure width of the scratch [13,31].

2.5.3. Live/dead staining experiment

dECMMA/GelMA was aseptically spread in a 12-well plate, and then RAW264.7 cells suspension were seeded at a density of 3×10^4 cells/cm^2. 1 mL of culture medium was added to each well. Calcein-AM and ethidium homodimer-1 (Live/Dead Cell Viability, Invitrogen, USA) were taken out 30 min in advance and placed at room temperature. The staining working solution was prepared following the provided instructions. On the third day of the culture, the initial culture medium was removed and gently washed with PBS three times. 200 μL of staining working solution was added to each well and covered the bottom of the plate. Incubated at room temperature in the dark for 30 min. Washed gently with PBS for three times, 3 min per time. Green fluorescence and red fluorescence were photographed at the same position using a fluorescence microscope and recorded [25,32].

2.5.4. Flow cytometry experiment

To investigate the effect of dECMMA/GelMA on the polarization of RAW264.7 cells into M1/M2 macrophages, flow cytometry was used to sort the M1/M2 macrophage populations. The specific steps were as follows: 300 μL of RAW264.7 cells suspension were seeded at a density of 3×10^4 cells/cm^2 in a 12-well plate and incubated for 12 h. Then, 1 mL of hydrogel extraction medium was added to each well. An equal amount of complete medium was added as a blank control. After 24 h of incubation, RAW264.7 cells were collected by trypsin digestion and resuspended in 100 μL of PBS containing 10 μg/mL of CD11b, PE-CD86, and APC-CD206 antibodies, respectively. After incubation at room temperature in the dark for 20 min, the light density of CD11b, PE-CD86, and APC-CD206 were detected using flow cytometry, and the data were analyzed using CytExpert software [32].

2.5.5. Angiogenesis assay and qPCR detection in vitro

A 96-well plate was prepared with 500 μL of serum-free DMEM medium in each well. 30 μL of dECMMA/GelMA was added to each well as the experimental group, while GelMA and blank groups were added as control groups. The plate was then allowed to sit undisturbed for 20 min at 37 °C. After photocuring into hydrogels, each well was seeded with 100 μL of cell suspension containing 1×10^4 human umbilical vein endothelial cells (HUVECs) and cultured in factor-free medium containing 0.1% bovine serum albumin to support HUVEC growth. The effects of the materials on the formation of tube-like structures similar to the lumen of blood vessels were observed under a microscope. After 24 h, HUVECs from each experimental group were collected, and total RNA was extracted using the RNAsimple Total RNA Extraction Kit. The expression of PDGF-BB, HIF1-α, and VEGF-related genes were detected by qPCR after reverse transcription and cDNA synthesis [30].

2.6. In vivo studies

A skin defect model (diameter 1 cm) was established by excising the skin of New Zealand rabbits (2 kg, male and female) from the Animal Service Center of Yangzhou University to create an animal model of skin injury. The wounds were covered with gauze (as a control group), GelMA, and dECMMA/GelMA, respectively. Four rabbits from each group were randomly selected and sacrificed 7 and 14 days at postoperative, and the wounds and surrounding tissues were removed and fixed in formalin solution. The samples were then embedded in paraffin, cut into 5 μm sections perpendicular to the tissue, and stained with hematoxylin-eosin (H&E) and Masson's trichrome for optical microscopy examination [18,19].

3. Statistical analysis

All data are presented as the mean ± SD and were analyzed using Origin 8.5 software (OriginLab Inc., USA) with a one-way ANOVA. Each experiment was repeated at least three times. *$p < 0.05$ and **$p < 0.01$ indicate statistical significance.

4. Results and discussion

4.1. Preparation and characterization of dECMMA/GelMA

Photocrosslinkable dECMMA and GelMA were used to form dECMMA/GelMA hydrogels via UV light crosslinking. It is well known that the miscibility of two polymers can be reflected in the morphology of their composite materials [33,34]. We examined the microstructure of GelMA and dECMMA/GelMA using SEM. The SEM results showed that both samples had a dense pore structure, indicating that the two materials were stable and the crosslinking was relatively uniform. The addition of dECMMA resulted in a reduction in the pores of the hydrogel, with a relatively uniform size and relatively continuous and compact pores, which can be attributed to the enhanced cross-linking between GelMA and dECMMA (Fig. 2A). The porous structure of these hydrogels is beneficial for the exchange of nutrients and promoting cell migration [35]. In this study, using FTIR detection, we observed that the absorption spectrum bands of amide infrared radiation (IR), including amide I (1631 cm^{-1}), amide II (1552 cm^{-1}), and amide A (3271 cm^{-1}), were characteristic peaks of infrared characterization of amide. Additionally, peaks at 1243 cm^{-1} and 1454 cm^{-1} were identified as the stretching vibration of C–N and the deformed vibration absorption peak of C–H of drugs, respectively (as shown in Fig. 2B). These results are consistent with previous reports [18,31]. Spectral features of GelMA and dECMMA/GelMA were also examined, and it was found that there were no significant changes in the absorption peaks, indicating that dECMMA/GelMA still possessed the basic chemical structure of a hydrogel [36]。

The swelling capacity of hydrogels is an important indicator of their performance, which represents their water storage ability. These traits enhance cell mobility and nutrient distribution, thereby promoting the healing of wounds within a humid microenvironment [28]. The change trend of the swelling rate of the two groups of hydrogels with time is shown in Fig. 2C. The swelling rate of hydrogel in the two groups changed similarly. In this study, GelMA and dECMMA/GelMA exhibited no statistically significant difference in their swelling capacity and both possessed good swelling performance. However, the initial swelling capacity of dECMMA/GelMA was weaker. We attribute this to the incorporation of dECMMA, which increased the crosslinking network of double bonds and hydrogen bonds, affecting the crosslinking density of the hydrogel. This led to reduced swelling ability, inhibiting rapid water

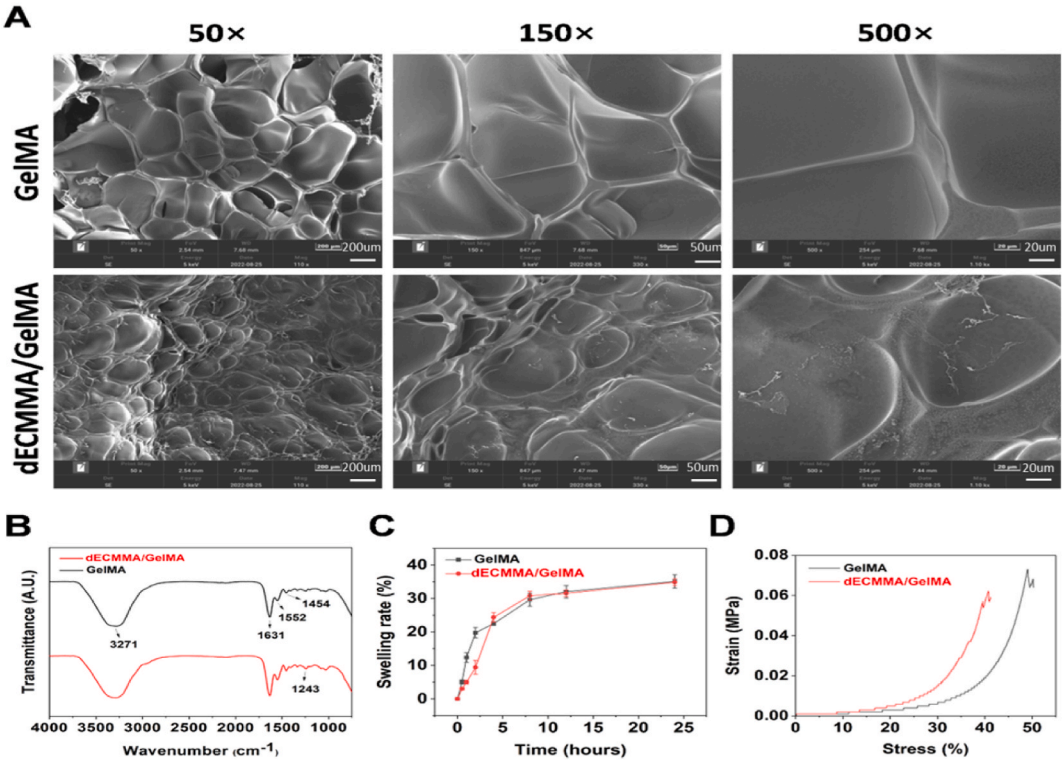

Fig. 2. A.SEM image of GelMA and dECMMA/GelMA; B. The infrared spectra of GelMA and dECMMA/GelMA; C. Swelling rate of GelMA and dECMMA/GelMA; D. Stress-strain curve of GelMA and dECMMA/GelMA.

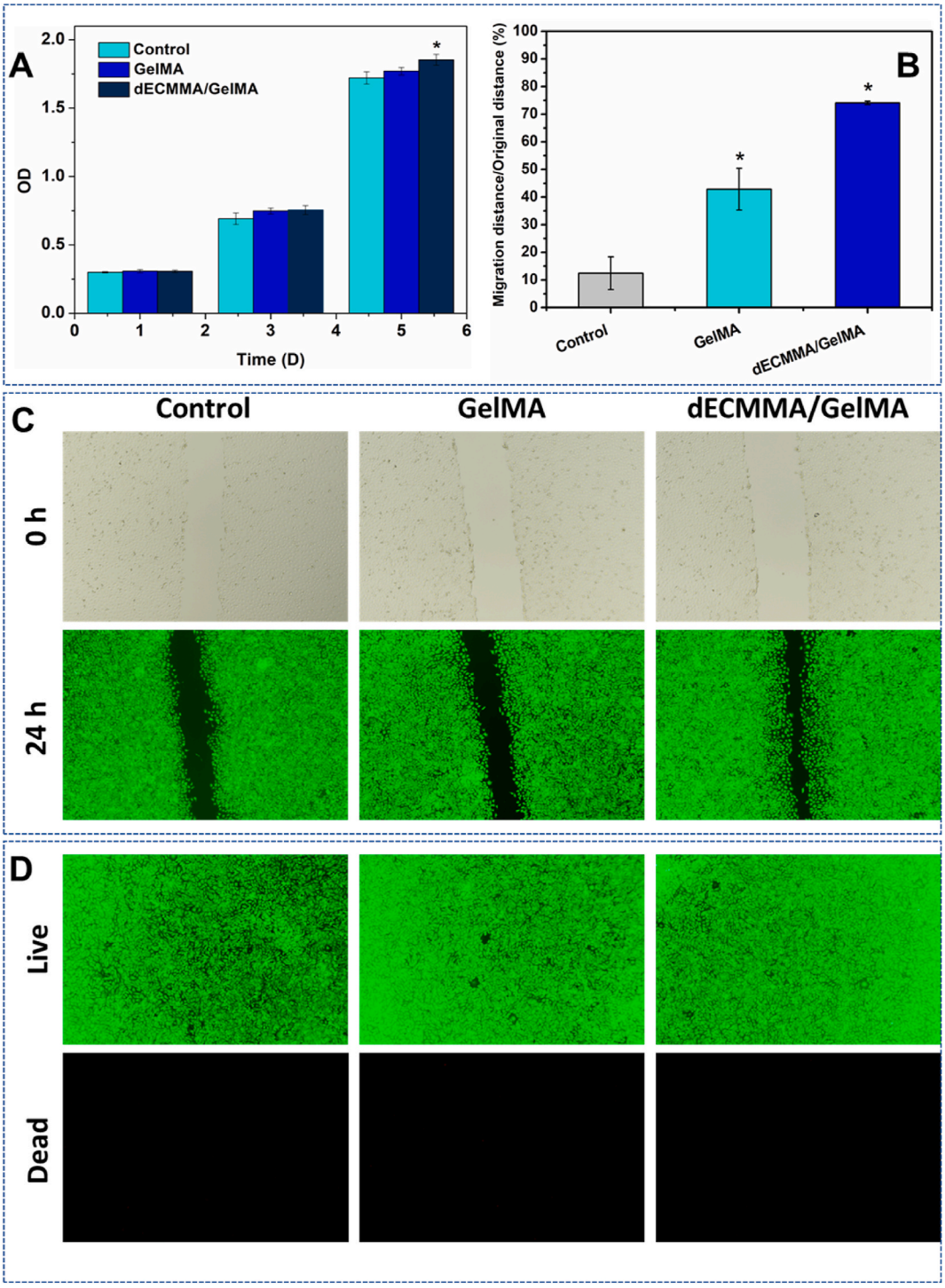

Fig. 3. Cell proliferation, migration, and toxicity testing. A. Analysis of RAW264.7 proliferation ability in the control group, GelMA group, and dECMMA/GelMA group after 1, 3, and 5 days of culture (*$p < 0.05$); B. Analysis of RAW264.7 migration ability in the control group, GelMA group, and dECMMA/GelMA group; C. Scratch test of RAW264.7 cells, showing that the migration ability of the dECMMA/GelMA group was superior to that of the GelMA group and the control group, with statistically significant differences (*$p < 0.05$); D. Live/dead staining was performed on RAW264.7 cells co-cultured for 3 days on the control group, GelMA group, and dECMMA/GelMA group. Green fluorescent cells represent live cells, while red fluorescent cells represent dead cells.

absorption. Concurrently, this alteration in the crosslinking structure correspondingly bolstered the mechanical properties, aligning with the observed changes in mechanical performance [37].

The stress-strain curves of the two groups of hydrogels are shown in Fig. 2D. The changes of stress with strain in the two groups of hydrogels are similar. However, the compressive modulus of dECMMA/GelMA is higher than that of GelMA. This may be because the hydrogen bond formed by the protein in the acellular matrix increases the modulus of the hydrogel [38]. A similar phenomenon is observed in composite hydrogels. For instance, the interaction between trehalose and polymer chains through hydrogen bonding creates an additional "polymer chain" layer on the fracture plane. This necessitates more energy to fracture a section of the polymer chain within a specific crack area. Additionally, there's a notable increase in mechanical dissipation near the crack tip. This can be attributed to the supplementary energy dissipation resulting from interactions akin to covalent bonds, such as hydrogen bonding [39].

4.2. *In vitro cell experiment*

The CCK-8 assay was used to quantitatively evaluate the proliferation of RAW264.7 cells cultured with or without hydrogels. After 1 and 3 days of co-culture, there were no significant differences in the OD values among the groups ($p > 0.05$). However, after 5 days of co-culture, the OD value of the dECMMA/GelMA group (1.85 ± 0.04) was significantly higher than that of the GelMA group (1.77 ±

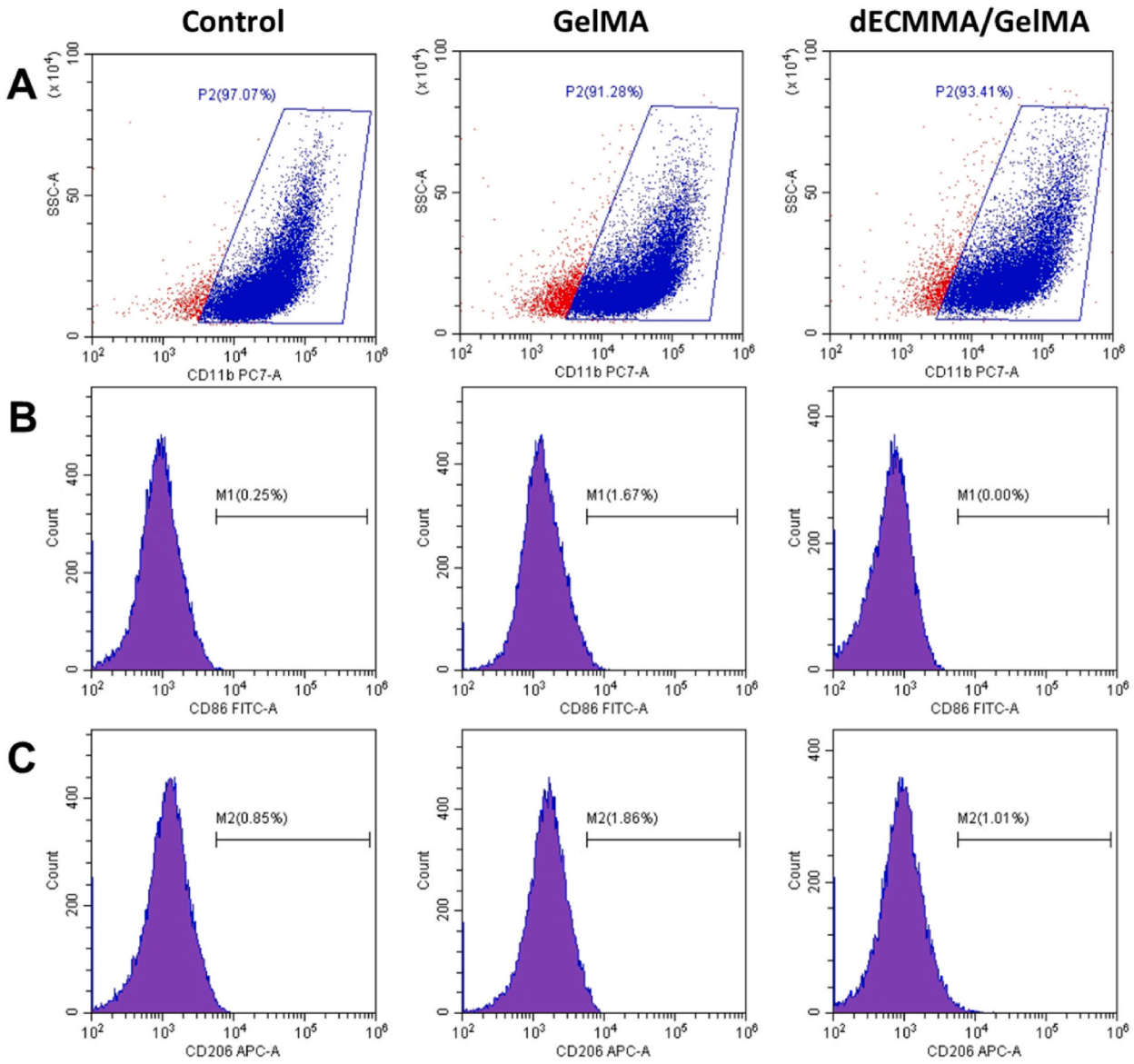

Fig. 4. Macrophage polarization was assessed using Raw264.7 cells cultured on the hydrogels. Flow cytometric analysis of the CD11b, CD86 and CD206 macrophages markers are shown in panels A, B and C, respectively.

0.03) and the control group (1.72 ± 0.04) (*p < 0.05), while there was no significant difference between the GelMA group and the control group (p > 0.05) (as shown in Fig. 3A). The dECMMA/GelMA group can promote cell proliferation, which we attribute primarily to its three-dimensional porous structure, which facilitates nutrient transport and cellular metabolism [40]. In addition, the presence of abundant active proteins and growth factors in dECMMA/GelMA is also one of the main reasons for promoting cell proliferation [18,21].

Cell migration is related to various physiological processes, such as cell proliferation, cell signaling, and cell-microenvironment interactions, regulating processes such as angiogenesis [31,37]. We compared cell migration by observing the relative position of cells on the surface of the hydrogels [41]. In the gap closure migration experiment (Fig. 3C), after 24 h of culture, cells around the wound began to migrate and the wound gradually closed. The dECMMA/GelMA group showed a significantly higher wound closure rate of 74.09 ± 0.60%, compared to the GelMA group (42.83 ± 7.57%) and the control group (12.45 ± 5.91%), with statistical significance (Fig. 3B, *p < 0.05). Good biocompatibility is a prerequisite for the clinical application of hydrogels. The ability of cells to survive and grow is crucial for tissue healing [13,19]. We used the Live/Dead assay to detect the cytotoxicity of dECMMA/GelMA hydrogels on RAW264.7 cells, and the results showed that RAW264.7 cells were viable on dECMMA/GelMA, with no significant cell death, indicating that dECMMA/GelMA has no significant cytotoxicity (Fig. 3D). Similar results were also confirmed by the CCK-8 assay.

4.3. Polarization of macrophages from M1 to M2 phenotype

Macrophages are the first responders to biological materials upon their entry into the human body, and they trigger a series of complex immune reactions to the materials. Therefore, it is crucial to assess the phenotypic changes of macrophages in response to the materials [25]. A significant feature of macrophages during the M1 or M2 polarization process is an increase in the expression of CD86 or CD206 [32]. Depending on the activation mode and the functional state after activation, macrophages can be polarized into two different phenotypes: pro-inflammatory macrophages of the M1 type and anti-inflammatory macrophages of the M2 type. If the content of M1 macrophages in the wound remains persistently high and cannot transition to the high M2 macrophages required for wound repair, then the sustained chronic inflammation will significantly delay tissue healing [29,32]. In this study, we assessed macrophage polarization by culturing Raw264.7 cells on hydrogels. Through flow cytometric analysis, we found that the materials significantly inhibited the expression of the CD11b marker in macrophages. The CD11b marker expression in the dECMMA/GelMA group was 93.41%, in the GelMA group was 91.28%, while in the blank group was 97.07%. CD11b can promote the development of bone marrow cells into the M1 macrophage subtype [42] , therefore, both materials can inhibit the phenotypic transformation of M1 macrophages, but the inhibition effect of the GelMA group was higher than that of the dECMMA/GelMA group (Fig. 4A). Analysis of CD86 subtype in M1 macrophages showed that the CD86 marker in the dECMMA/GelMA group was 0%, in the GelMA group was 1.67%, and in the control group was 0.25%, indicating that the dECMMA/GelMA group had a certain inhibitory effect on the

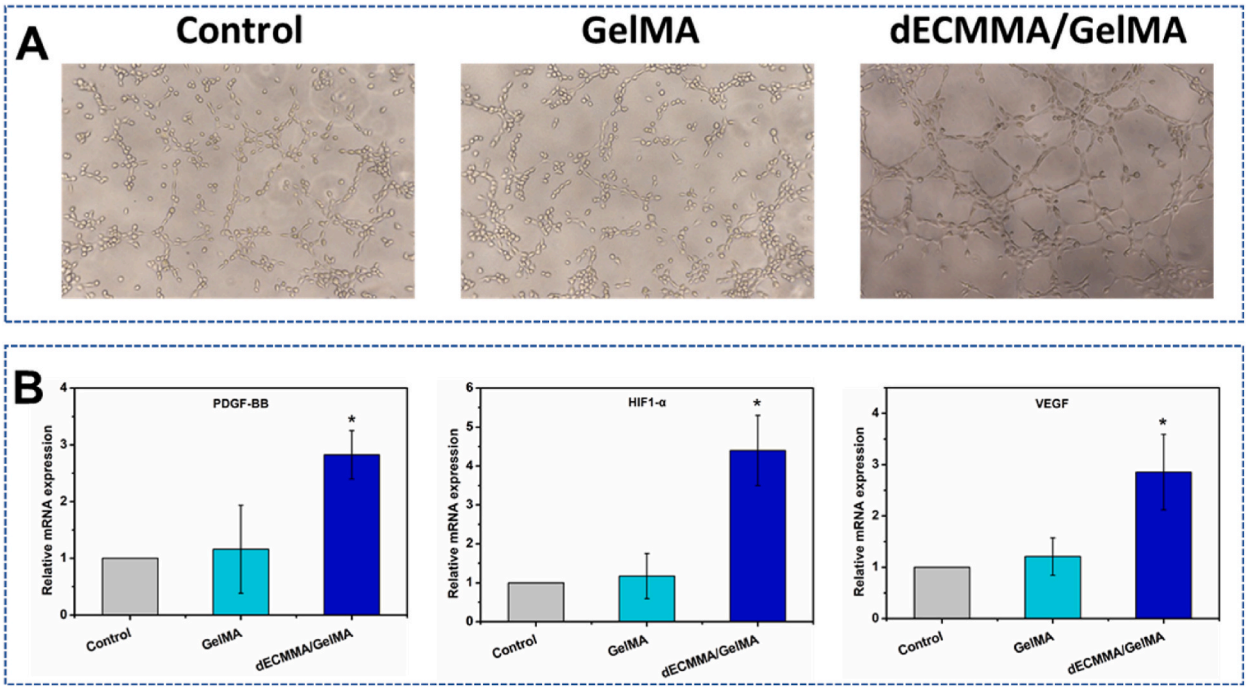

Fig. 5. Assessing the angiogenic capacity of hydrogels. A. HUVECs cultured with blank control group, GelMA group, and dECMMA/GelMA group for 24 h; B. Statistical analysis for the expression levels of PDGF-BB, HIF1-α, and VEGF.

phenotypic differentiation of M1 macrophages (Fig. 4B). Furthermore, analysis of CD206 subtype in M2 macrophages showed that the CD206 marker in the dECMMA/GelMA group was 1.01%, in the GelMA group was 1.86%, and in the control group was 0.85%, indicating that the ECMMA/GelMA group and the GelMA group had a certain promoting effect on the phenotypic differentiation of M2

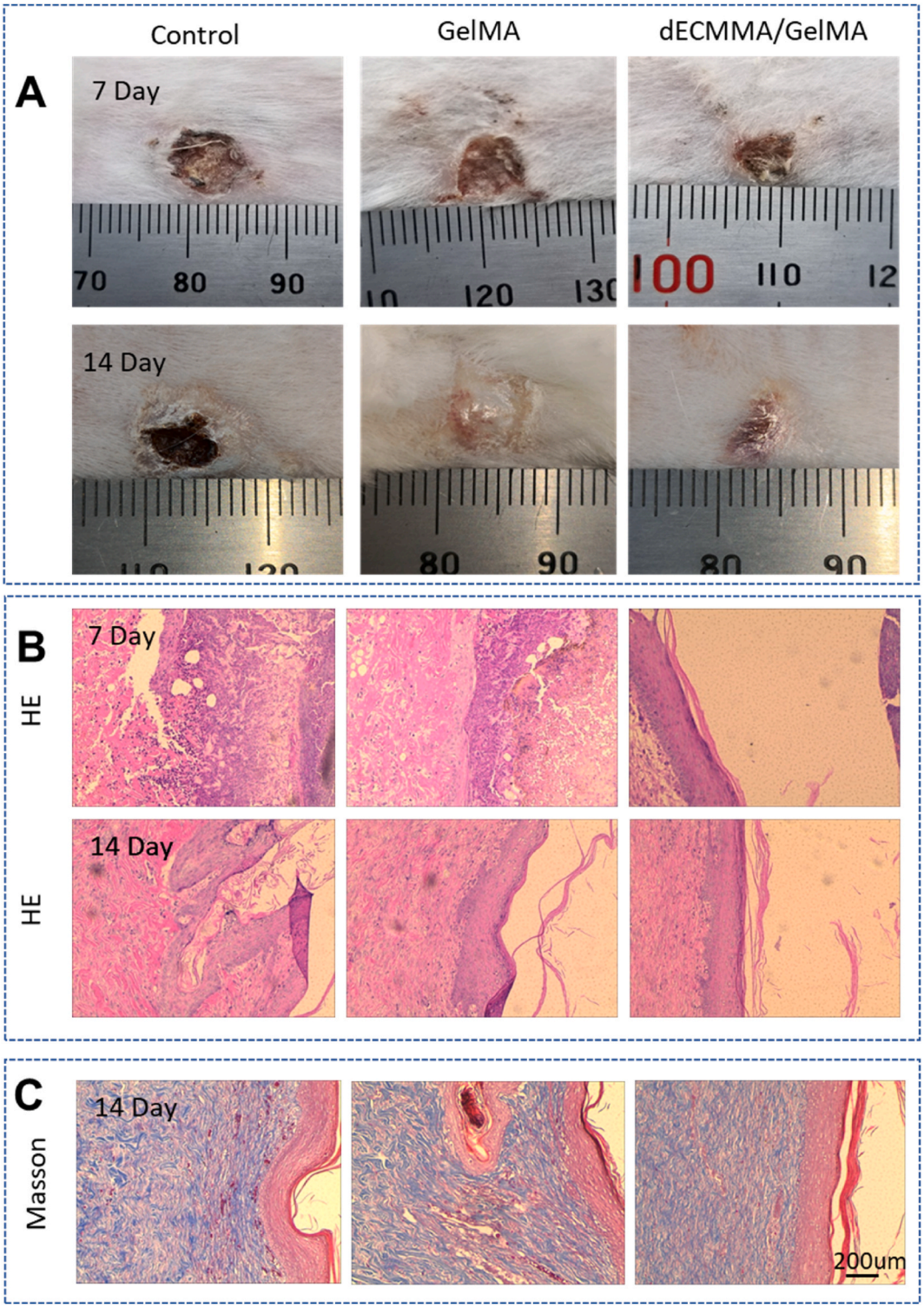

Fig. 6. Evaluation of in vivo performance: A) Wound healing of rabbit skin defect model; B) Histological Analysis with Hematoxylin and Eosin (H&E) Staining; C) Masson staining of defect tissue treated with gauze (as control), GelMA and dECMMA/GelMA after surgery.

macrophages, with the promoting effect of the GelMA group being higher than that of the dECMMA/GelMA group (Fig. 4C). However, the effect of the GelMA group on both M1 and M2 phenotypes was not clear and evenly positive. On the contrary, the dECMMA/GelMA group showed a clear inhibitory effect on the M1 phenotype and a promoting effect on the M2 phenotype, demonstrating a clear anti-inflammatory effect.

4.4. The angiogenic capacity of dECMMA/GelMA

Angiogenesis and neovascularization play a critical role in the process of wound healing [43]. PDGF-BB promotes mitosis, cell proliferation, migration, and angiogenesis in various cells, playing an important role in tissue injury and repair. PDGF-BB and HIF1-α can promote the secretion of VEGF factors and upregulation of VEGF expression in endothelial cells, inducing morphological changes in angiogenesis and inducing neovascularization [44]. Neovascularization can improve microcirculation at the wound site, providing necessary oxygen and nutrients for injury repair and playing an important role in the wound healing process [13,28,30].Fig. 5A shows that after 24 h, the dECMMA/GelMA group formed a primary capillary-like network of endothelial cells, while the blank group and the GelMA group only formed some indistinct tubular structures. HUVECs from each experimental group were collected after 24 h, and total RNA was extracted from the cells using the RNAsimple Total RNA Extraction Kit. The cDNA was then synthesized and qPCR was performed for detection. As shown in Fig. 5B, the expression of PDGF-BB, HIF1-α, and VEGF in the dECMMA/GelMA group were significantly higher than that in the blank group and the GelMA group, with values of 2.85 ± 0.74, 4.4 ± 0.90, and 2.82 ± 0.43, respectively. The differences were statistically significant (Fig. 5B, $^*p < 0.05$). dECMMA/GelMA has been shown to promote high expression of PDGF-BB, HIF1-α and VEGF-related genes, indicating good angiogenic ability [44]. Based on existing research results, it has been proven that amniotic membrane can promote wound healing and neovascularization [26]. Therefore, we believe that the growth factor composition of dECM may explain the formation of neovascularization.

4.5. In vivo skin defect repair

In order to assess the effectiveness of dECMMA/GelMA as a functional dressing for wounds, we employed a full-thickness rabbit wound model and compared the outcomes of wounds treated with dECMMA/GelMA to those treated with GelMA-only and untreated wounds [3,18,30]. During the experiment, the New Zealand white rabbits recovered well after surgery, and survived without the use of antibiotics. The wound gradually healed. Fig. 6A illustrates the overall images of the control group, GelMA group, and dECMMA/-GelMA group after 7 and 14 days post-operation. Observation of skin recovery at 7 days post-operation highlighted that wound healing in the control and GelMA groups was comparatively less effective than that observed in wounds treated with the dECMMA/GelMA composite. The reduction in wound area was notably greater in the dECMMA/GelMA group compared to the control and GelMA groups. Upon assessing overall recovery at 14 days, a substantial decrease in wound area was noted across all rabbit groups. Nevertheless, the wound areas in the control and GelMA groups remained larger than those in the dECMMA/GelMA group, indicating the superior wound healing rate achieved through the dECMMA/GelMA composite treatment. At 7 and 14 days after surgery, the dECMMA/GelMA group had relatively more epithelial cell nail spikes, good cell stratification, and a transition from a single layer to a multilayered epithelial keratinization. The GelMA group showed a gradual increase in the number and arrangement of epithelial cell layers, with more fibroblasts and inflammatory cells. The blank group had a relatively high number of inflammatory cells, poor healing, uneven thickness, and no obvious multilayer keratinization. Masson staining can color collagen fibers a deep blue, with a darker shade indicating a greater collagen content. This method is employed to assess the level of collagen deposition in the wound area [19,30]. Therefore, to further investigate the recovery of the skin, we performed Masson staining on the regenerated tissue of the wound 14 days after surgery (Fig. 6B). Consistent with the H&E results, the wound healing of the dECMMA/GelMA group was superior to that of the GelMA group, with orderly collagen fiber arrangement, while the blank group showed poor recovery after 14 days, with uneven thickness, disordered and sparse collagen fiber arrangement, and more infiltration of inflammatory cells (Fig. 6C). Our results suggest that dECMMA/GelMA can promote the healing of damaged skin tissue.

Skin tissue engineering has emerged as a novel approach for repairing soft tissue injuries of the skin [8]. ECM can activate cellular responses such as cell migration, proliferation, and differentiation by binding to cell surface receptors [18,19]. Therefore, the design and preparation of biomaterials that mimic the composition and structure of ECM are crucial for tissue regeneration [14,19]. By grafting modification with methacrylate (MA), we combined natural decellularized ECM (dECM) with GelMA to construct a dECM-MA/GelMA composite hydrogel, which exhibited excellent biocompatibility and bioactivity. It can simulate the ECM microenvironment as an active matrix and promote the rapid healing of defective tissues by controlling cell migration, proliferation, and differentiation. Our in vitro observations have shown that dECMMA/GelMA promotes cell proliferation, migration, angiogenesis, and has anti-inflammatory effects. Furthermore, our in vivo research results have demonstrated that dECMMA/GelMA can promote re-epithelialization on wound surfaces, facilitating early deposition of ECM collagen and promoting wound healing.

However, the mechanism of action of dECMMA/GelMA and its associated tissue healing signaling pathways remain unclear in this study [9]. Moreover, the fabrication process and optimization of the theoretical performance of this composite hydrogel require further investigation [4]. Additionally, further studies are required in other large animal models, such as pig models, in order to facilitate clinical translation in the future years.

5. Conclusion

In this study, a novel bioactive dressing made of dECMMA/GelMA was developed through grafting modification of dHAM and

GelMA, followed by photopolymerization. This bioactive dressing was designed to maintain a moist microenvironment for promoting cell viability and proliferation. The unique characteristic of dECMMA/GelMA allows for the continuous formation of a biomimetic ECM microenvironment that is conducive to wound healing. It up-regulates the expression of PDGF-BB, HIF1-α, and VEGF for angiogenesis, promotes re-epithelialization, anti-inflammatory capacity, and collagen deposition. Therefore, dECMMA/GelMA could be an excellent bioactive wound dressing that enhances healing quality. However, further biocompatibility tests and in vivo experiments with additional animals need to be conducted in our follow-up studies before clinical usage.

Ethical statement

All experiments were conducted in accordance with applicable laws and guidelines, following the institutional guidelines of Yangzhou University. The discarded placenta was the source of dHAM, and informed consent was obtained from the pregnant woman (Ethics No. 2021-YKL03-G026). All animal procedures were conducted in strict compliance with the Guidelines for the Care and Use of Laboratory Animals established by Yangzhou University and were duly approved by the Animal Ethics Committee of the same institution (Ethics No. 202103089).

Author contribution statement

Qiang Zhang; Wei Liu: Conceived and designed the experiments; Contributed reagents, materials, analysis tools or data.
Lifa Chen; JueLan Ye: Performed the experiments; Analyzed and interpreted the data; Wrote the paper.
Chong Gao; Fei Deng: Performed the experiments.

Data availability statement

Data will be made available on request.

Declaration of competing interest

The authors declare that they have no known competing financial interests or personal relationships that could have appeared to influence the work reported in this paper.

Acknowledgements

This work was supported by Yangzhou Science and Technology Bureau (YZ2021076), Jiangsu Commission of Health (H2019035).

References

[1] Y.H. Shan, L.H. Peng, X. Liu, X. Chen, J. Xiong, J.Q. Gao, Silk fibroin/gelatin electrospun nanofibrous dressing functionalized with astragaloside IV induces healing and anti-scar effects on burn wound, Int. J. Pharm. 479 (2) (2015) 291–301.
[2] X. Lei, L. Qiu, M. Lan, X. Du, S. Zhou, P. Cui, R. Zheng, P. Jiang, J. Wang, J. Xia, Antibacterial photodynamic peptides for staphylococcal skin infection, Biomater. Sci. 8 (23) (2020) 6695–6702.
[3] A.R. Ahmady, K. Razmjooee, S. Saber-Samandari, D. Toghraie, Fabrication of chitosan-gelatin films incorporated with thymol-loaded alginate microparticles for controlled drug delivery, antibacterial activity and wound healing: in-vitro and in-vivo studies, Int. J. Biol. Macromol. 223 (Pt A) (2022) 567–582.
[4] K. Razmjooee, Azin Rashidy Ahmady, Naghmeh Arabzadeh, b Sara Ahmadi, S. Saber-Samandari, D. Toghraie, Synthesis of Gelatin/Polyacrylamide/Carboxymethyl chitosan triple-network hydrogels and evaluation of their properties for potential biomedical applications, Mater. Sci. Eng. B 295 (2023), 116597.
[5] R. Yang, G. Song, L. Wang, Z. Yang, J. Zhang, X. Zhang, S. Wang, L. Ding, N. Ren, A. Wang, X. Yu, Full solar-spectrum-driven antibacterial therapy over hierarchical Sn(3) O(4)/PDINH with enhanced photocatalytic activity, Small 17 (39) (2021), e2102744.
[6] Y. Liang, Y. Liang, H. Zhang, B. Guo, Antibacterial biomaterials for skin wound dressing, Asian J. Pharm. Sci. 17 (3) (2022) 353–384.
[7] K. Vig, A. Chaudhari, S. Tripathi, S. Dixit, R. Sahu, S. Pillai, V.A. Dennis, S.R. Singh, Advances in skin regeneration using tissue engineering, Int. J. Mol. Sci. 18 (4) (2017).
[8] M. Persinal-Medina, S. Llames, M. Chacon, N. Vazquez, M. Pevida, I. Alcalde, S. Alonso-Alonso, L.M. Martinez-Lopez, J. Merayo-Lloves, A. Meana, Polymerizable skin hydrogel for full thickness wound healing, Int. J. Mol. Sci. 23 (9) (2022).
[9] F. Karami, S. Saber-Samandari, Synthesis and characterization of a novel hydrogel based on carboxymethyl chitosan/sodium alginate with the ability to release simvastatin for chronic wound healing, Biomed. Mater. 18 (2) (2023).
[10] Y. Liang, X. Zhao, T. Hu, B. Chen, Z. Yin, P.X. Ma, B. Guo, Adhesive hemostatic conducting injectable composite hydrogels with sustained drug release and photothermal antibacterial activity to promote full-thickness skin regeneration during wound healing, Small 15 (12) (2019), e1900046.
[11] B. Yang, J. Song, Y. Jiang, M. Li, J. Wei, J. Qin, W. Peng, F.L. Lasaosa, Y. He, H. Mao, J. Yang, Z. Gu, Injectable adhesive self-healing multicross-linked double-network hydrogel facilitates full-thickness skin wound healing, ACS Appl. Mater. Interfaces 12 (52) (2020) 57782–57797.
[12] S. Ganguly, P. Das, E. Itzhaki, E. Hadad, A. Gedanken, S. Margel, Microwave-synthesized polysaccharide-derived carbon dots as therapeutic cargoes and toughening agents for elastomeric gels, ACS Appl. Mater. Interfaces 12 (46) (2020) 51940–51951.
[13] X. Zhao, Q. Lang, L. Yildirimer, Z.Y. Lin, W.G. Cui, N. Annabi, K.W. Ng, M.R. Dokmeci, A.M. Ghaemmaghami, A. Khademhosseini, Photocrosslinkable gelatin hydrogel for epidermal tissue engineering, Adv. Healthcare Mater. 5 (1) (2016) 108–118.
[14] K. Yue, G. Trujillo-de Santiago, M.M. Alvarez, A. Tamayol, N. Annabi, A. Khademhosseini, Synthesis, properties, and biomedical applications of gelatin methacryloyl (GelMA) hydrogels, Biomater 73 (2015) 254–271.
[15] K. Da Silva, P. Kumar, S.F. van Vuuren, V. Pillay, Y.E. Choonara, Three-dimensional printability of an ECM-based gelatin methacryloyl (GelMA) biomaterial for potential neuroregeneration, ACS Omega 6 (33) (2021) 21368–21383.
[16] Y.C. Chen, R.Z. Lin, H. Qi, Y. Yang, H. Bae, J.M. Melero-Martin, A. Khademhosseini, Functional human vascular network generated in photocrosslinkable gelatin methacrylate hydrogels, Adv. Funct. Mater. 22 (10) (2012) 2027–2039.

[17] M. Neufurth, X. Wang, H.C. Schroder, Q. Feng, B. Diehl-Seifert, T. Ziebart, R. Steffen, S. Wang, W.E.G. Muller, Engineering a morphogenetically active hydrogel for bioprinting of bioartificial tissue derived from human osteoblast-like SaOS-2 cells, Biomater 35 (31) (2014) 8810–8819.
[18] Q. Zhang, C. Chang, C. Qian, W. Xiao, H. Zhu, J. Guo, Z. Meng, W. Cui, Z. Ge, Photo-crosslinkable amniotic membrane hydrogel for skin defect healing, Acta Biomater. 125 (2021) 197–207.
[19] S. Xiao, C. Xiao, Y. Miao, J. Wang, R. Chen, Z. Fan, Z. Hu, Human acellular amniotic membrane incorporating exosomes from adipose-derived mesenchymal stem cells promotes diabetic wound healing, Stem Cell Res. Ther. 12 (1) (2021) 255.
[20] S.V. Murphy, A. Skardal, L.J. Song, K. Sutton, R. Haug, D.L. Mack, J. Jackson, S. Soker, A. Atala, Solubilized amnion membrane hyaluronic acid hydrogel accelerates full-thickness wound healing, Stem Cell Transl Med 6 (11) (2017) 2020–2032.
[21] J.J.D. Henry, L. Delrosario, J. Fang, S.Y. Wong, Q. Fang, R. Sievers, S. Kotha, A. Wang, D. Farmer, P. Janaswamy, R.J. Lee, S. Li, Development of injectable amniotic membrane matrix for postmyocardial infarction tissue repair, Adv. Healthcare Mater. 9 (2) (2020), e1900544.
[22] B. Farhadihosseinabadi, M. Farahani, T. Tayebi, A. Jafari, F. Biniazan, K. Modaresifar, H. Moravvej, S. Bahrami, H. Redl, L. Tayebi, H. Niknejad, Amniotic membrane and its epithelial and mesenchymal stem cells as an appropriate source for skin tissue engineering and regenerative medicine, Artif. Cells, Nanomed. Biotechnol. 46 (sup2) (2018) 431–440.
[23] K. Tang, J. Wu, Z. Xiong, Y. Ji, T. Sun, X. Guo, Human acellular amniotic membrane: a potential osteoinductive biomaterial for bone regeneration, J. Biomater. Appl. 32 (6) (2018) 754–764.
[24] L.F. Jorge, J.C. Francisco, N. Bergonse, C. Baena, K.A.T. Carvalho, E. Abdelwahid, J.R.F. Neto, L.F.P. Moreira, L.C. Guarita-Souza, Tracheal repair with acellular human amniotic membrane in a rabbit model, J Tissue Eng Regen Med 12 (3) (2018) e1525–e1530.
[25] H. Liu, Z. Zhou, H. Lin, J. Wu, B. Ginn, J.S. Choi, X. Jiang, L. Chung, J.H. Elisseeff, S. Yiu, H.Q. Mao, Synthetic nanofiber-reinforced amniotic membrane via interfacial bonding, ACS Appl. Mater. Interfaces 10 (17) (2018) 14559–14569.
[26] Y. Zheng, S. Ji, H. Wu, S. Tian, Y. Zhang, L. Wang, H. Fang, P. Luo, X. Wang, X. Hu, S. Xiao, Z. Xia, Topical administration of cryopreserved living micronized amnion accelerates wound healing in diabetic mice by modulating local microenvironment, Biomater 113 (2017) 56–67.
[27] M.T. Sultan, J.Y. Jeong, Y.B. Seo, O.J. Lee, H.W. Ju, H.J. Park, Y.J. Lee, J.S. Lee, S.H. Kim, C.H. Park, Fabrication and characterization of the porous duck's feet collagen sponge for wound healing applications, J. Biomater. Sci. Polym. Ed. 29 (7–9) (2018) 960–971.
[28] R. Jin, Y. Cui, H. Chen, Z. Zhang, T. Weng, S. Xia, M. Yu, W. Zhang, J. Shao, M. Yang, C. Han, X. Wang, Three-dimensional bioprinting of a full-thickness functional skin model using acellular dermal matrix and gelatin methacrylamide bioink, Acta Biomater. 131 (2021) 248–261.
[29] W. Kim, H. Lee, J. Lee, A. Atala, J.J. Yoo, S.J. Lee, G.H. Kim, Efficient myotube formation in 3D bioprinted tissue construct by biochemical and topographical cues, Biomater 230 (2020), 119632.
[30] C. Qian, T. Xin, W. Xiao, H. Zhu, Z.J.N.A.M. Ge, Vascularized silk electrospun fiber for promoting oral mucosa regeneration, NPG Asia Mater. 12 (39) (2020).
[31] X.M. Sun, Q. Lang, H.B. Zhang, L.Y. Cheng, Y. Zhang, G.Q. Pan, X. Zhao, H.L. Yang, Y.G. Zhang, H.A. Santos, W.G. Cui, Electrospun photocrosslinkable hydrogel fibrous scaffolds for rapid in vivo vascularized skin flap regeneration, Adv. Funct. Mater. 27 (2) (2017).
[32] P. Qiu, M. Li, K. Chen, B. Fang, P. Chen, Z. Tang, X. Lin, S. Fan, Periosteal matrix-derived hydrogel promotes bone repair through an early immune regulation coupled with enhanced angio- and osteogenesis, Biomater 227 (2020), 119552.
[33] D. Luo, W. Zhen, C. Dong, L. Zhao, Performance and multi-scale investigation on the phase miscibility of poly(lactic acid)/amided silica nanocomposites, Int. J. Biol. Macromol. 177 (2021) 271–283.
[34] A. Skardal, M. Devarasetty, H.W. Kang, I. Mead, C. Bishop, T. Shupe, S.J. Lee, J. Jackson, J. Yoo, S. Soker, A. Atala, A hydrogel bioink toolkit for mimicking native tissue biochemical and mechanical properties in bioprinted tissue constructs, Acta Biomater. 25 (2015) 24–34.
[35] S. Wang, Y. Xiong, J. Chen, A. Ghanem, Y. Wang, J. Yang, B. Sun, Three dimensional printing bilayer membrane scaffold promotes wound healing, Front. Bioeng. Biotechnol. 7 (2019) 348.
[36] W. Li, Y. Lan, R. Guo, Y. Zhang, W. Xue, Y. Zhang, In vitro and in vivo evaluation of a novel collagen/cellulose nanocrystals scaffold for achieving the sustained release of basic fibroblast growth factor, J. Biomater. Appl. 29 (6) (2015) 882–893.
[37] J. Liu, M. Qu, C. Wang, Y. Xue, H. Huang, Q. Chen, W. Sun, X. Zhou, G. Xu, X. Jiang, A dual-cross-linked hydrogel patch for promoting diabetic wound healing, Small 18 (17) (2022), e2106172.
[38] J. Boublik, H. Park, M. Radisic, E. Tognana, F. Chen, M. Pei, G. Vunjak-Novakovic, L.E. Freed, Mechanical properties and remodeling of hybrid cardiac constructs made from heart cells, fibrin, and biodegradable, elastomeric knitted fabric, Tissue Eng. 11 (7–8) (2005) 1122–1132.
[39] Z. Han, P. Wang, Y. Lu, Z. Jia, S. Qu, W. Yang, A versatile hydrogel network-repairing strategy achieved by the covalent-like hydrogen bond interaction, Sci. Adv. 8 (8) (2022), eabl5066.
[40] M. Koning, M.C. Harmsen, M.J. van Luyn, P.M. Werker, Current opportunities and challenges in skeletal muscle tissue engineering, J Tissue Eng Regen Med 3 (6) (2009) 407–415.
[41] C. Schmitz, B.S. Eastwood, S.J. Tappan, J.R. Glaser, D.A. Peterson, P.R. Hof, Current automated 3D cell detection methods are not a suitable replacement for manual stereologic cell counting, Front. Neuroanat. 8 (2014) 27.
[42] E.T. Richardson, S. Shukla, N. Nagy, W.H. Boom, R.C. Beck, L. Zhou, G.E. Landreth, C.V. Harding, ERK signaling is essential for macrophage development, PLoS One 10 (10) (2015), e0140064.
[43] C. Noishiki, S. Yuge, K. Ando, Y. Wakayama, N. Mochizuki, R. Ogawa, S. Fukuhara, Live imaging of angiogenesis during cutaneous wound healing in adult zebrafish, Angiogenesis 22 (2) (2019) 341–354.
[44] C. Del Rosario, M. Rodriguez-Evora, R. Reyes, A. Delgado, C. Evora, BMP-2, PDGF-BB, and bone marrow mesenchymal cells in a macroporous beta-TCP scaffold for critical-size bone defect repair in rats, Biomed. Mater. 10 (4) (2015), 045008.